# Textile dyes loaded chitosan nanoparticles: characterization, biocompatibility and staining capacity

Eduardo M Costa[a*]; Sara Silva[a]; Mariana Veiga[a]; Patricia Baptista[a]; Freni K Tavaria[a]; Manuela E Pintado[a]

[a] Universidade Católica Portuguesa, CBQF - Centro de Biotecnologia e Química Fina – Laboratório Associado, Escola Superior de Biotecnologia, Rua Diogo Botelho 1327, 4169-005 Porto, Portugal

*corresponding author: emcosta@porto.ucp.pt

Abstract

Textile dyeing is a hazardous and toxic process. While traditionally it has been managed through effluent treatment, new approaches focused upon improving the dyeing process are gaining relevance. In this work, we sought to obtain, for the first time, an eco-friendly chitosan-nanoparticle based textile dyeing method. To that end, yellow everzol and navy blue itosperse loaded chitosan nanoparticles were produced and their capacity to dye textiles and cytotoxicity towards human skin cells were evaluated. The results obtained showed that it was possible to obtain nanoencapsulated dyes through ionic gelation with an average entrapment efficacy above 90%. Nanoparticles presented a positive surface charge and sizes between 190 and 800 nm with yellow everzol NPs occurring via ionic interactions while navy blue itosperse NPs were formed through hydrogen bonds. Furthermore, the produced dye NPs presented no cytotoxicity towards HaCat cells and presented staining percentages reaching 17.60% for a viscose/wool blend.

**Keywords:** Chitosan nanoparticles; reactive dye; disperse dye; nanoencapsulation; skin biocompatibility; textile dyeing.

## 1. Introduction

Conventional textile dyeing techniques are quite hazardous as chemicals are used in large quantities and wastewaters need to be cleaned before discharge. Furthermore, the synthetic dyes used nowadays are reported to be toxic, and possibly carcinogenic and mutagenic, with the possible toxic effects varying from contact dermatitis and skin allergies to tumours and heart problems (Alver, Bulut, Metin, & Çiftçi, 2017; Cao et al., 2014; Luo & Van Ooij, 2002; Nayak, Isloor, Moslehyani, Ismail, & Ismail, 2018; Shahid ul, Shahid, & Mohammad, 2013; Shahidi, Wiener, & Ghoranneviss, 2013; Wasim, Sagar, Sabir, Shafiq, & Jamil, 2017). The traditional approach to this problem has been through effluent treatment with the textile industry focusing on means to remediate the polluted wastewaters [8]. Nowadays, a new approach has risen where adjuvants are being used to improve textile dyeability, in an effort to reduce the quantity of dye required in the dyeing process. Among these adjuvants are chitosan (CS) and its nanoparticles (NPs).

Chitosan is one of the most promising biopolymers as it is a polycationic polysaccharide obtained from partial deacetylation of chitin with high biocompatibility, biodegradability and with no toxicity which is approved by the FDA for topical application, particularly in wound healing (A. Kumar, Vimal, & Kumar, 2016). Chitosan NPs production through ionic gelation is attractive as it allows for reproducible production of NPs, with small sizes and narrow population distribution, in a mild environment (*e.g.* water) and doesn't require the usage of any organic solvent or toxic cross-linking agent (Banerjee, Mitra, Kumar Singh, Kumar Sharma, & Maitra, 2002; Bugnicourt & Ladavière, 2016). Application of chitosan NPs in the textile industry is already on the way with previous works using them as finishing agents capable of providing antimicrobial activity (Ali, Rajendran, & Joshi, 2011), enhance the breaking strength, shrink-proof and wrinkle-resistance properties (Lu, Chen, Lin, Wang, & Yang, 2010; Yang, Wang, Huang, & Hon, 2010) or as enhancers of textile dyeing (Cheung, Szeto, & McKay, 2009). Additionally, chitosan nanoparticles are a perfect candidate for textile dyeing, as they are known to interact with various fabrics, have proven interaction with dyes, reduced toxicity and their larger surface area make for a better candidate than the chitosan molecule itself (Ali et al., 2011; Hu, Zhang, Chan, & Szeto, 2006; Wang et al., 2011).

Considering all of the above, we hypothesized that is possible to stain textiles using a chitosan NPs based, chemical adjuvant and salt-free, procedure. To do so yellow everzol (reactive dye) and navy blue itosperse (disperse dye) loaded chitosan NPs were produced, through the ionic gelation, and the obtained nanoencapsulated dyes (NDs) structure, size and charge were characterized. Following that, the cytotoxicity of the obtained NDs relatively to human keratinocytes was

evaluated and their capacity to dye various synthetic and natural fabrics through a novel, adjuvant and salt-free process, was ascertained.

## 2. Materials & Methods

### *2.1. Sources of chemicals and solutions preparation*

Low molecular weight chitosan (LMW) (Sigma-Aldrich, St. Louis, USA) was previously characterized by Gullon et al. (2016) and presents a deacetylation degree (DD) of 90.10 ± 5.76% and a molecular weight (MW) of 123.01 ± 5.32 kDa. Sodium Tripolyphosphate (TPP) was obtained from Sigma-Aldrich (St. Louis, USA). Reactive (yellow everzol (YE)) and disperse (navy blue itosperse (IN)) textile dyes were kindly donated by Aquitex – Acabamentos Químicos Têxteis S.A. and were prepared at 10 mg/mL using ultra-pure water (Millipore SIM FILTER, Massachusetts, USA) and stirred until complete dissolution.

### *2.2. Nanoencapsulated dyes production*

Nanoencapsulated dyes were produced using the ionic gelation methodology through adaptation of the procedure described by Costa et al. (2017). Briefly, LMW chitosan was dissolved at 2 mg/mL in acetic acid that was 1.75x more concentrated and the pH value was adjusted to 4-5 with NaOH. TPP was used at chitosan to TPP relation of 7:1. Yellow everzol and navy blue itosperse were used at various concentrations (0.1, 0.5, 1 and 5 mg/mL) dissolved in deionized water. The process began with the addition of 4 mL of chitosan, placed under stirring at 500 rpm, to which a mixture of dye and TPP (1 and 2 mL, respectively) were gently added dropwise, at room temperature. At the end of the process, the NDs were characterized and then frozen and freeze-dried for posterior use in the FTIR and cytotoxicity assays.

### *2.3. Nanoencapsulated dyes characterization*

#### *2.3.1. Particle size and charge*

The NDs suspensions were analyzed concerning their physical properties by dynamic light scattering (DLS) using a Malvern Instruments NanoZSP (Worcestershire, UK). The measured parameters were particle size (PS), polydispersity index (PdI) and zeta potential (ZP). All assays were performed using a disposable folded capillary cell (Malvern, Worcestershire, UK), with a 90 ° laser angle and at room temperature (25 °C). Size values were determined based on intensity distribution. All assays were performed in sextuplicate.

#### *2.3.2. Determination of entrapment efficiency of NDs*

Nanoencapsulated dyes solutions were centrifuged at 13000 rpm, 20 °C, during 10 min. Sample supernatants were then recovered and the optical density (OD) measured at the $\lambda_{max}$ of each dye and unentrapped dye content in aqueous solution was determined using a standard curve drawn using the test dye concentrations and their respective ODs. The entrapment efficiency determined according to the following formula:

Entrapment % = (Dye Content $_{(unentrapped\ dye)}$/ Initial Dye Content) x 100

All measures were performed in quadruplicate.

*2.3.3. FTIR-ATR analysis*

The spectra of chitosan, TPP and chitosan nanoparticles was obtained with a Fourier transform infrared spectrometer (FTIR) (PerkinElmer Spectrum-100), with a horizontal attenuated total reflectance (ATR) accessory, with a diamond/ZnSe crystal. All spectra were acquired with 128 scans and 32 $cm^{-1}$ resolution, in the region of 4500 to 450 $cm^{-1}$. Three replicates were collected for each sample.

*2.3.4. Cytotoxicity evaluation*

*2.3.4.1. Cell line growth conditions*

Human keratinocyte cell line (HaCat) was obtained from Cell Line Services (Oppenheim, Denmark). The cells were cultured, at 37 °C in a humidified atmosphere of 95% air and 5% $CO_2$, as monolayers using Dulbecco's Modified Eagle's Medium (DMEM) with 4.5 g/L glucose, L-glutamine without pyruvate (Lonza, Verviers, Belgium) containing 10% (v/v) fetal bovine serum (FBS, Biowest, Nuaillé, France) and 1% (v/v) Penicillin-Streptomycin-Fungizone (Lonza, Verviers, Belgium). Cells were used between passages 35 and 41.

*2.3.4.2. XTT assay*

Cytotoxicity evaluation was performed accordingly to the ISO 10993-5:2009 standard (ISO, 2009) using the XTT ( 2,3-Bis(2-methoxy-4-nitro-5-sulfophenyl)-2H-tetrazolium-5-carboxanilide inner salt) viable dye. Briefly, HaCat cells were seeded at 1 x $10^5$ cells/mL in the wells of a 96 well microplate and allowed to adhere. After 24 h, the media was removed and the cells washed with PBS. Following this, media with NDs and void NPs at 5 mg/mL were added. Simultaneously, two controls were accessed: one with 10% DMSO and other with sterile water. After 24h, 25 µL of XTT working solution were added to each well and the cells were incubated, in the dark, for 2 h. The optical density (OD) at 485 nm was then measured using a microplate reader (FLUOstar, OPTIMA, BMG Labtech,

Ortenberg, Germany). All assays were performed in quintuplicate. The results were expressed in percentage of cell metabolism inhibition according to the equation below:

Cell inhibition % = 100- ($OD_{(sample)}$/ $OD_{(control)}$)×100

*2.4. NDs textile dying*

Nanoencapsulated dyes' capacity to dye different textiles was screened through adaptation of the pad-dry-cure procedure previously described by Tavaria et al. (2012). Briefly, 4 cm cotton circles were dipped in NDs solution (5 mg/mL) during 10 min. Impregnated samples were then dried at 100 °C for 10 min, rinsed to remove non-adhered material, cured at 100 °C for 10 min and then air-dried. Initially, dying was judged qualitatively by observation of visible dying of the assayed textile and results were given by the presence or absence of colour in the fabric. For dyed samples, the NDs uptake percentage was evaluated through the weight difference of the cotton samples before and after dyeing.

*2.5. Statistical analysis*

Statistical analysis was performed using IBM SPSS Statistics v21.0.0 (New York, USA) software. As the data followed a normal distribution, One-way ANOVA coupled with Turkey's post hoc test was used to assess the differences between the results observed with differences being considered significant for p-values below 0.05.

## 3. Results

*3.1. Particle size and charge*

Analysing the size results of the produced NDs (**Figure 1**) it is possible to see a clear size difference between the encapsulated dyes.

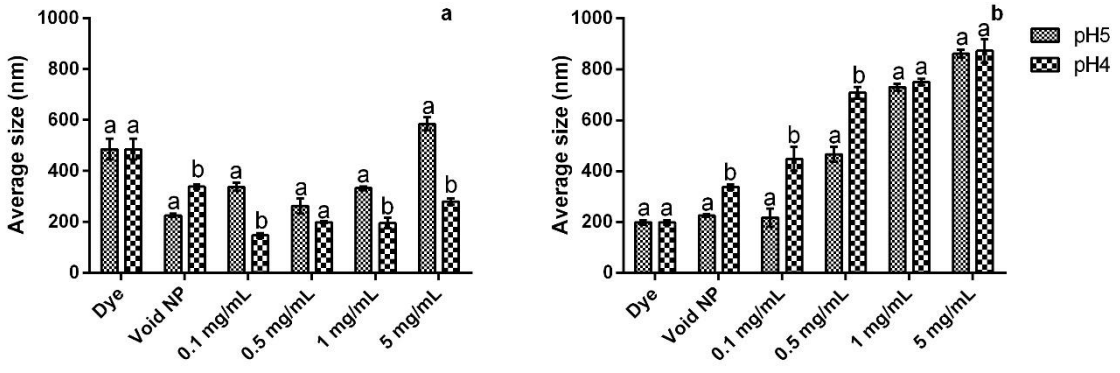


**Figure 1 - Average size (nm) of the different nanoencapsulated dyes produced at the concentrations tested. A) Yellow everzol NDs; B) Itosperse Navy NDs. Different letters represent the statistically significant ($p < 0.05$) differences found between conditions assayed.**

In general, the NDs produced with yellow everzol (NDYE) (**Figure 1a**) presented smaller average size than those produced with navy blue itosperse (NDIN) (**Figure 1b**) and while for the first the pH value was a statistically significant ($p < 0.05$) factor in particle size for the latter, this influence was only statistically significant ($p < 0.05$) at the lower concentrations tested. When considering the data obtained for NDYE only (**Figure 1a**), it interesting to see that, at pH4, all NDs produced were significantly smaller ($p < 0.05$) than the unloaded dye (void NPs). In fact, when considering the influence of the pH value upon NDYE production it is easy to see that for all tested concentrations the average size obtained at pH 4 was significantly ($p < 0.05$) smaller than the one obtained at pH 5. From a size standpoint, it is interesting to denote that with the increase in dye concentration there was a gradual increase in particle size, with only the large particles obtained at 0.1 mg/mL (pH 5) deviating from this behaviour. On the other hand, the data obtained for NDIN (**Figure 1b**) shows a completely different pattern of encapsulation. First, all NDs produced presented a significantly ($p < 0.05$) larger average size than the un-encapsulated dye (except for 0.1 mg/mL at pH 5, for which the difference was not statistically significant ($p > 0.05$)). Second, and as previously referred, in the NDs production, the pH only had a statistically significant ($p < 0.05$) effect at the two lowest concentrations tested and contrary to what was observed for NDYE the smaller particles were produced at pH 5. Lastly, from a size standpoint, it bears notice the steep increase in particle size observed with the increase in dye concentration, which is best reflected by the fact that the particles obtained at 5 mg/mL of navy blue itosperse reaching almost a micrometre scale (*ca.* 870 nm of average size) and being between 2.57 and 4.5 times larger than the un-encapsulated dye and the void NPs.

When regarding the average charge of the produced NDs the obtained results can be seen in **Figure 2**.

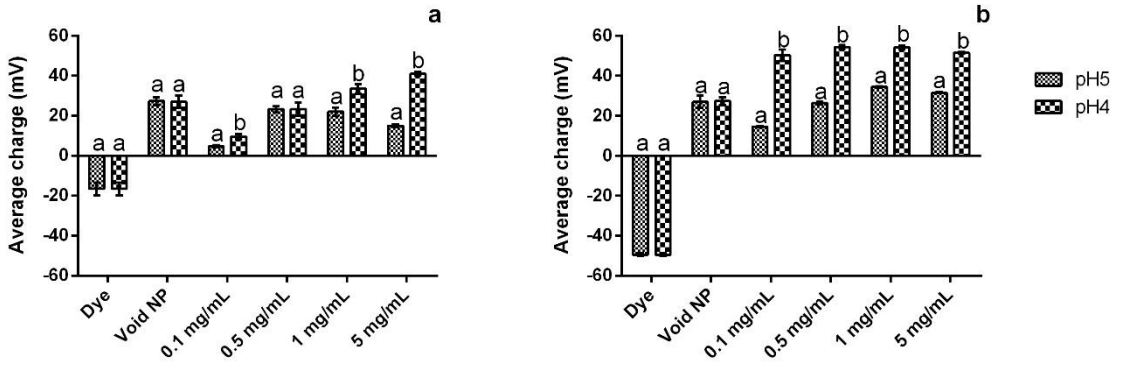


**Figure 2 - Average charge (mV) of the different nanoencapsulated dyes produced at the concentrations tested. A) Yellow everzol NDs; B) Itosperse Navy NDs. Different letters represent the statistically significant ($p < 0.05$) differences found between conditions.**

Overall, it is possible to see that despite the un-encapsulated dyes possessing a negative average charge all of the produced NDs presented a positive surface charge. Additionally, it is possible to see that for both NDs the production pH value played a significant ($p < 0.05$) role in the NDs average charge, as particles produced at pH 4 presented, in average, a significantly ($p < 0.05$) higher charge than the ones produced at pH 5. When regarding the results obtained for NDYE (**Figure 2a**) it is possible to see a clear dichotomic behaviour between the tested pH values, as at pH 4 the increase in dye concentration led to an increase in particle charge while at pH 5 the same increase led to a decrease in particle charge (except for the transition from 0.1 to 0.5 mg/mL of YE). Additionally, while for pH 4 from 0.5 mg/mL onwards the surface charge values obtained were equal or significantly ($p < 0.05$) higher than that registered for the void NPs for pH 5, the same was not observed as despite the dye concentration used, the particle surface charge was always significantly ($p < 0.05$) lower than that registered for the void NPs. When considering the data obtained for NDIN (**Figure 2b**), it is possible to see that at both pH values tested, the increase in dye concentration led to an increase in the particles overall surface charge. In fact, for pH 5, from 1 mg/mL onwards, and for pH 4, in all tested concentrations, the NDs produced had a significantly ($p < 0.05$) higher surface charge than the one registered for the void NPs. Furthermore, and similarly to what was observed for NDYE, the NDs produced at pH 4 had a significantly ($p < 0.05$) higher surface charge than the ones produced at pH 5.

### *3.2. Dye entrapment*

The results obtained regarding the entrapment efficiency of the nanoencapsulation process can be seen in **Figure 3**.

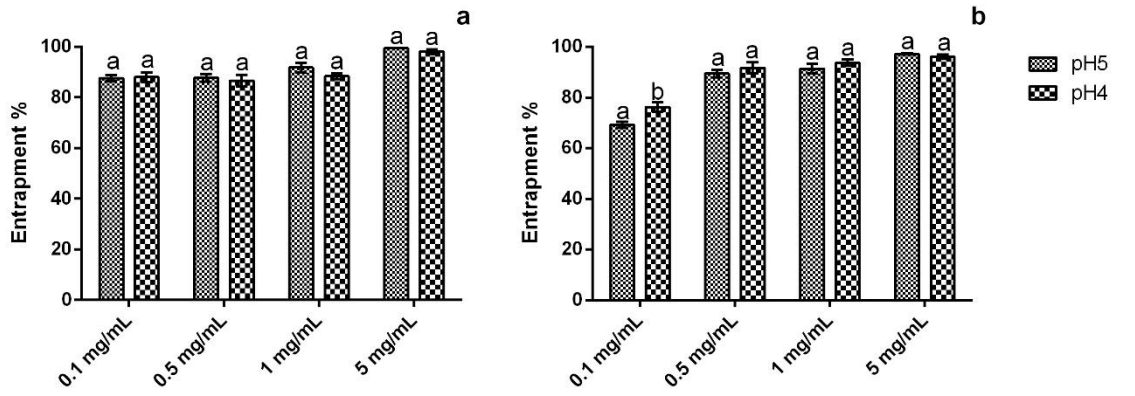


**Figure 3 - Entrapment % of the different nanoencapsulated dyes produced at the concentration tested. a) Yellow everzol NDs; b) Itosperse Navy NDs. Different letters represent the statistically significant ($p < 0.05$) differences found between conditions.**

Overall, it is interesting to see that the lowest entrapment percentage registered was of *ca.* 70% and that, in general, the pH value did not significantly ($p < 0.05$) influence dye entrapment. Furthermore, it is also apparent the direct relation between entrapment percentage and dye concentration as a steady increment of the first was registered with the concomitant increase of the latter. On an individual analysis of the results obtained it is possible to see that for NDYE (**Figure 3a**) there was little variation of the entrapment % between all tested concentrations. In fact, only at the highest dye concentration tested, the entrapment % obtained was significantly ($p < 0.05$) higher than those registered at the previous concentrations. However, it must be taken into account the high entrapment % registered in all tested conditions as it varied between 88 % and 98%. On the other hand, for NDIN (**Figure 3b**) higher variations of entrapment % were observed, with the results obtained at 0.1 mg/mL of dye being significantly ($p < 0.05$) lower than those registered in the remaining conditions; while the results obtained at 5 mg/mL of dye being significantly ($p < 0.05$) higher than those obtained in the lower concentrations tested. Additionally, it also stands to notice the steep increase in entrapment % with the increase in dye concentration and that while the highest entrapment % obtained was similar to that registered for NDYE (*ca.* 97% relatively to *ca.* 98%) the lowest concentration obtained was significantly ($p < 0.05$) lower than the one recorded for the yellow everzol NDs (*ca.* 70% relatively to *ca.* 88%).

### *3.3. FTIR*

When analyzing the FTIR spectra of the NDs (**Figure 4**) it is possible to see clear similarities and differences between these and the spectra of the void chitosan NPs (**Figure 4a**).

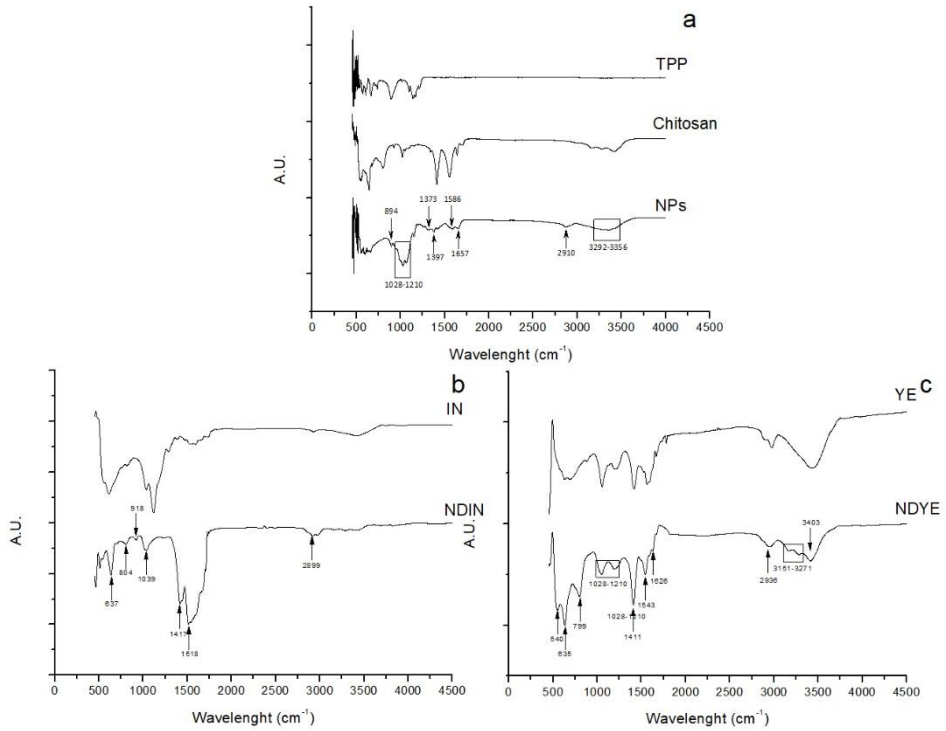


**Figure 4 - FTIR spectra of void chitosan NPs (a), Itosperse Navy NDs (NDIN) (b) and Yellow Everzol NDS (NDYE) (c).**

For NDIN (**Figure 4B**), of the 7 peaks observed, 4 were characteristic of chitosan NPs while the remaining 3 were new. Chitosan NPs characteristic peaks were observed at 2899 $cm^{-1}$, which corresponds to the asymmetric and symmetric $CH_2$ vibrations of the pyranose ring, at 1518 $cm^{-1}$, which indicates that chitosan-TPP crosslinking occurred through interaction between TPP and the amino groups of chitosan, and the ones at 1039 and 918 $cm^{-1}$ correspond to the COH stretching, C–N and N-H vibrations indicative of an interaction between CS and TPP, respectively. Interestingly, the other 3 peaks all report alterations related to the chitosan carbon structure as the one identified at 1417 $cm^{-1}$ relates to the α-$CH_2$ bending and the ones at 804 and 637 $cm^{-1}$ correspond to C-H bending and deformation, respectively. Similarly, for NDYE (**Figure 4C**) in the FTIR spectra obtained of the 12 peaks identified 8 are characteristic of chitosan NPs, while the remaining 4 find no correspondence with the void NPs spectra. The chitosan NPs characteristic peaks observed are the ones corresponding to the squared area and are between 3271 and 3151 $cm^{-1}$, which correspond to the enhanced hydrogen bond in NPs, the one at approximately 2936 $cm^{-1}$ which represents the asymmetric and symmetric $CH_2$ vibration attributed to the pyranose ring, the peak 1626 $cm^{-1}$, which represents the C=O stretching in NPs, the one 1543 $cm^{-1}$, which represents the chitosan-TPP crosslinking was performed through interaction between TPP and the amino groups, and the ones

in the second squared area (1028 to 1210 $cm^{-1}$) where the merging of characteristic chitosan and TPP absorption peaks can be found. Similarly to what was observed for NDIN, with the exception of the peak registered at 540 $cm^{-1}$, the peaks registered at 1411, 799 and 635 $cm^{-1}$ correspond to alterations to the chitosan carbon structure, with the first representing the α-$CH_2$ bending and the second and the third demonstrating C-H bending and deformation. On the other hand, the outlier peak (540 $cm^{-1}$) represents a weak S-S disulphide connection a result of the sulfonated groups known to be present in reactive dyes (Georgiou, Melidis, Aivasidis, & Gimouhopoulos, 2002; Haider, Majeed, Williams, Safdar, & Zhong, 2017; Joseph, Sangeetha, & Gomathi, 2016; Robinson, McMullan, Marchant, & Nigam, 2001).

*3.4. Cytotoxicity evaluation*

When considering the cytotoxicity of the NDs it is possible to see (**Figure 5**) that the encapsulation process led to a significant loss of toxicity of the textile dye, as both NDYE and NDIN led to the preservation of cell viability while the un-encapsulated dyes diminished cell viability by *ca.* 100 (YE) and 73% (IN) well above the 30% limit defined by the ISO 10993-5:2009 standard (ISO, 2009).

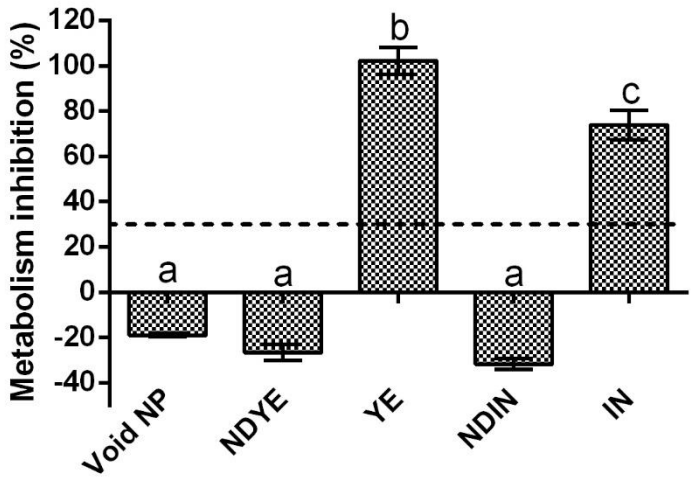


**Figure 5 – Evaluation of the cytotoxicity of Yellow Everzol (NDYE) and Itosperse Navy (NDIN) NDs. Different letters represent the statistically significant ($p < 0.05$) differences found between conditions. The dotted line represents the 30% cytotoxicity limit as defined by the ISO 10993-5:2009 standard.**

It is interesting to note that the encapsulation of the textile dyes led to an apparent, but statistically insignificant ($p > 0.05$) increase in cellular metabolism, relatively to the void NPs.

*3.5. NDs textile dying*

The results obtained regarding the screening of the produced NDs capacity to dye different types of textiles using the pad-dry-cure methodology can be seen in **Table 1**.

**Table 1 – Nano-encapsulated and free dyes textile dyeing screening results. Results given qualitatively.**

| | Cotton | Viscose\wool blend | Viscose\lycra blend | Cotton\Lyocell blend | Wool\Polyamide blend | Polyester |
|---|---|---|---|---|---|---|
| YE | Yes | No | No | No | No | No |
| NDYE | Yes | Yes | Yes | Yes | Yes | Yes |
| IN | No | No | No | No | No | Yes |
| NDIN | Yes | Yes | Yes | Yes | Yes | Yes |

Overall, it is interesting to see that there was no dye-substrate affinity as the produced NDs were capable of dyeing both synthetic (polyester, lycra), natural textiles, irrespectively of these being of protein (wool) or cellulose (cotton) based, and blends of fabrics equally. Following these results, the average NDs uptake to various fabrics was calculated and the results obtained can be seen in **Figure 6**.

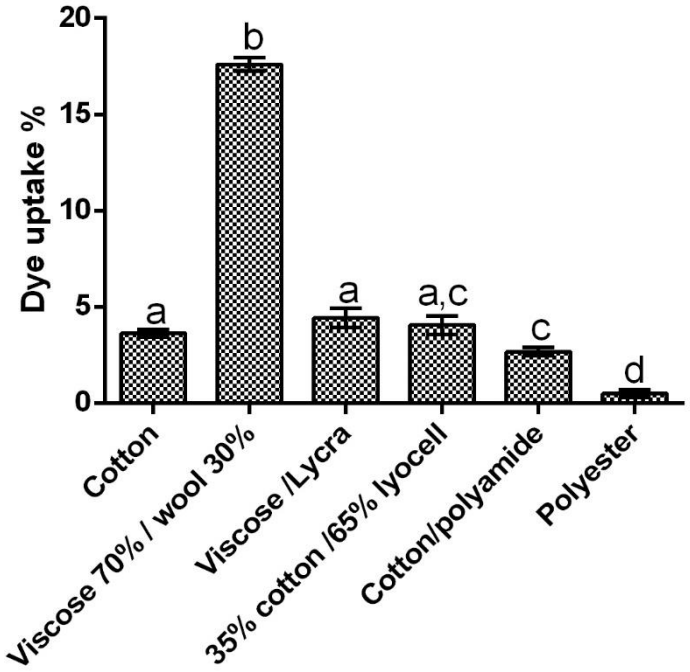


**Figure 6 - Nanoencapsulated dyes average uptake percentages for different fabrics tested. Different letters represent statistically significant differences found ($p < 0.05$).**

Overall, the NDs average uptake percentage varied between 0.51 and 17.60%. On a closer look, viscose/wool blend and polyester uptake percentages were significantly ($p < 0.05$) higher and lower, respectively, than the ones registered for remaining fabrics. For these fabrics, while there were no statistically significant ($p > 0.05$) differences registered between cotton, viscose/lycra and the

cotton/lyocell blends the uptake percentages obtained for these fabrics were significantly ($p < 0.05$) higher than the one registered for cotton/polyamide blend.

## 4. Discussion

The process of ionic gelation is one of the easiest ways to develop chitosan nanoparticles as it's a one-shot synthesis procedure executed at mild environmental conditions. Furthermore, these nanoparticles present the ability to incorporate various compounds in their matrix, shielding them from external environments and agents. The incorporation of hydrophilic compounds, as the ones used in this work, via ionic gelation process is particularly adequate as they can be mixed with the initial chitosan or TPP solution, depending on their charge, originating nanoparticles with the compounds entrapped in their polymer matrix or adsorbed to the particle surface (Bugnicourt & Ladavière, 2016; Wu, Yang, Wang, Hu, & Fu, 2005). Despite previous work focusing mainly on using chitosan nanoparticles as a means of dye removal from wastewaters (Hu et al., 2006; Zhou, Jin, Liu, Liang, & Shang, 2011) inklings of chitosan NPs potential for the development of green, chemical-free processes for textile dyeing already exist in the literature as Hebeish, Sharaf, and Farouk (2013) and Ali et al. (2011) reported that a chitosan NPs finish led to higher adsorption of negatively charged dyes.

From a nanoencapsulation perspective is interesting to see that the different nature of the target molecule (reactive dyes have sulfuric moieties while disperse dyes have nitro and amino moieties) had overall effects upon the particles size and charge. For reactive dyes, such as yellow everzol, interaction with chitosan NPs has been described as being of electrostatic nature, most likely via ionic interactions, through the interaction of its sulfuric moieties with chitosan amino groups (Cao et al., 2014; Momenzadeh, Tehrani-Bagha, Khosravi, Gharanjig, & Holmberg, 2011). Furthermore, this interaction has been described as being strongly pH value-dependent as lower values lead to higher protonation degree of chitosan's amino groups which in turns will allow a higher interaction between this groups and the dyes sulfuric moieties (Cheung et al., 2009; Zhou et al., 2011). While in theory, this would mean that lower pH values would facilitate the reactive dyes entrapment this is not true, as Momenzadeh et al. (2011) showed that at pH values under 4 there will be a gradual protonation of the dye's sulfuric groups. On the other hand, disperse dyes lacking sulfuric groups, interact with chitosan NPs via their nitro and amine moieties and thus, are passible of being influenced by the solutions overall pH value (Boardman, Lad, Green, & Thornton, 2017). All of these interactions were on full display on the NDs size results obtained as for yellow everzol NDs behaviour was strongly pH value-dependent, with the lower values presenting better results, while for the navy blue itosperse the pH value was not as significant. Interestingly enough, the high

increase in particle size observed for NDIN is a common behaviour in NPs loading, as the size of the nanoparticle has been described as increasing significantly with the size or/and molecular weight of the encapsulated compound (Gan & Wang, 2007). However, as could be seen in **Figure 1** the yellow everzol molecule presented a significantly higher size than the itosperse dye used and thus it should originate larger size particles. A potential explanation for this discrepancy lays in the work of Shajahan et al. (2017), who showed that reactive dyes are adsorbed to the chitosan molecules on the surface of the NPs, and thus despite being entrapped are not fully encapsulated which leads to smaller particle sizes.

The adsorption of reactive dyes to the NPs surface also helps in explaining the low surface charge of NDYE, as the sulphuric groups of the particles adsorbed to the surface possess negative charge, and finds some concordance in the literature as Gan and Wang (2007) showed that NPs loading with electronegative compounds may lead to a reduction in surface charge and Alver et al. (2017) showed that chitosan NPs loaded with a reactive dye had a negative zeta potential. On the other hand, the high surface charge observed for NDIN may be a result of the encapsulation process on itself, as in disperse dyes nitro and amine moieties will interact with chitosan hydroxyl groups (Boardman et al., 2017) resulting, probably, in greater exposure of the positively charged amino groups on the nanoparticle surface. When considering the entrapment efficiency of the produced NDs, it must be taken into account that the presence of functional groups on the target compounds has an important role in their ability to interact and to be incorporated into the chitosan nanoparticle (Loh, Schneider, Carter, Saunders, & Lim, 2010). As such, and considering the known interactions between the tested compounds and chitosan NPs, the high entrapment % obtained could be somewhat expected. However, while previous works (Alver et al., 2017; Boardman et al., 2017; Shajahan et al., 2017) reported high entrapment percentages (83% to 98%) for reactive dyes, thus supporting the data here obtained, the same cannot be said for disperse dyes with entrapment percentages reported being generally lower than those obtained for reactive dyes (Boardman et al., 2017; Shajahan et al., 2017).

The FTIR results obtained showed that for the void NPs, the interaction at the molecular level between chitosan and TPP stands in line with previous works, as the acquired spectra confirmed the complex formation between chitosan and TPP through electrostatic interactions (Galante et al., 2016; Haider et al., 2017; Hashad, Ishak, Fahmy, Mansour, & Geneidi, 2016). Similarly, the data obtained for NDYE fully supports the assumption that reactive dyes are, at least partly, adsorbed to the NPs surface (Shajahan et al., 2017), as a S-S disulphide connection typical of reactive dyes (Georgiou et al., 2002; Robinson et al., 2001) was identified in the spectra. Additionally, the alterations to the chitosan carbon structure found maybe a result of encapsulated dye molecules

ionic interaction with chitosan's amino groups as previously described (Cao et al., 2014; Momenzadeh et al., 2011). On the other hand, for NDIN the differences found in the spectra, relatively to void NPs, are mostly focused upon bends and deformations of C-H and $CH_2$ thus lending credence to the theory that disperse dyes interaction with chitosan NPs occurs through hydrogen bonds with chitosan hydroxyl groups (Boardman et al., 2017).

Synthetic textiles dyes have been widely characterized as being carcinogenic and hazardous to the human health with possible toxic effects varying from dermatitis and skin allergies to tumours and heart problems (Alver et al., 2017; Nayak et al., 2018; Wasim et al., 2017). Previous works have shown that reactive dyes at concentrations as low as 0.01 mg/mL are capable of reducing HaCat cells viability by almost 90% and that their $IC_{50}$ can be of only 0.155 mg/mL (Chaudhari, Paul, Dhotre, & Kodam, 2017; Jha, Jobby, & Desai, 2016). Similarly, disperse dyes have been described as decreasing the cellular viability of HepG2 cells (Tsuboy et al., 2007). As such, the high toxicity observed in this work for both dye molecules was expected. On the other hand, the lack of toxicity observed for the void chitosan NPs comes with previous works (Nogueira et al., 2013). Interestingly enough the loading of both highly toxic dyes into a biocompatible matrix did not lead to any apparent loss of cellular viability of HaCat cells. Considering that chitosan NPs have been described as being capable of protecting loaded compounds from the outside environment (S. P. Kumar, Birundha, Kaveri, & Devi, 2015), it is highly probable that entrapped compounds lack the capacity to interact with the outside environment and, in this case, exert any cytotoxic effect upon the HaCat cells. Lastly, but not least, the textile dyeing screening results obtained showed that both NDs were capable of dyeing all tested textiles, regardless of them being synthetic (polyester, lycra), natural textiles or blends of fabrics, while the free compounds were only capable of dyeing cotton (yellow everzol) and polyester (navy blue itosperse). The results obtained for the free molecules come inline the existing body of work as, traditionally, reactive dyes are only capable of dyeing cotton and other cellulosic fibres while on the other hand, disperse dyes are used with polyester fibres (Burkinshaw & Salihu, 2018). Additionally, the apparent lack of fabric specificity observed for the NDs may be a direct result of chitosan's NPs and the tested fabrics nature. As the loaded NDs produced were positively charged and the zeta potential of textile fibres is negative (Ramesh Kumar & Teli, 2007) we hypothesize that the when the dye loaded NDs are placed in contact with the textiles there won't be any interaction between the dye and the textile and the textile impregnation will be due to an electrostatic interaction between the positively charged NDs and the negatively charged fabric surface thus circumventing traditional dyeing limitations. When considering the uptake percentages registered, textiles dyed through conventional techniques report dye fixation percentages between 50-80 % lower percentages can still be obtained, as dyes can also react with

water hydroxyl groups instead of the cellulose hydroxyl groups (Ahmed, 2005; Khatri, Peerzada, Mohsin, & White, 2015; Smith, 2005; Tissera, Wijesena, & de Silva, 2016). On the other hand, whereas the highest NDs uptake registered in this work was of only 17.6% the process employed allowed the application of a reactive dye to various fabrics, of synthetic and natural origin, and not only cotton. Additionally, it was environmentally friendly, as it occurred at room temperature without the addition of salt or any chemical adjuvant, and was relatively fast as, from NDs production to textile dying only took, at most, 45 min.

## 5. Conclusions

Overall, this work showed that our hypothesis was correct and that it was possible to dye textile fabrics using only textile dye loaded chitosan NPs. The proposed nanoencapsulation procedure, using the chitosan TPP ionic gelation method, obtained extremely high entrapment efficiencies at the tested concentrations. Additionally, despite reactive and disperse dyes having high cytotoxicity the nanoencapsulated dyes were not cytotoxic towards HaCat cells. Moreover, this work showed, for the first time, a NDs based, environment friendly, textile dyeing procedure that bypassed traditional dye-fabric specific. These results, while promising, still require further assays to better understand the relationship between the nanoencapsulated dyes and textiles, to ascertain if the NDs developed retained some of the chitosan's biological potential and if NDs are capable of imparting biological activity to textiles.

## Acknowledgements

This work was supported by National Funds from FCT (grant numbers UID/Multi/50016/2019, SFRH/BD/90867/2012 and SFRH/BDE/103957/2014) and QREN-ANI (project 17819).

## References

Ahmed, N. S. E. (2005). The use of sodium edate in the dyeing of cotton with reactive dyes. *Dyes and Pigments,* 65(3), 221-225.

Ali, S. W., Rajendran, S., & Joshi, M. (2011). Synthesis and characterization of chitosan and silver loaded chitosan nanoparticles for bioactive polyester. *Carbohydrate Polymers,* 83(2), 438-446.

Alver, E., Bulut, M., Metin, A. Ü., & Çiftçi, H. (2017). One step effective removal of Congo Red in chitosan nanoparticles by encapsulation. *Spectrochimica Acta Part A: Molecular and Biomolecular Spectroscopy,* 171, 132-138.

Banerjee, T., Mitra, S., Kumar Singh, A., Kumar Sharma, R., & Maitra, A. (2002). Preparation, characterization and biodistribution of ultrafine chitosan nanoparticles. *International Journal of Pharmaceutics,* 243(1-2), 93-105.

Boardman, S. J., Lad, R., Green, D. C., & Thornton, P. D. (2017). Chitosan hydrogels for targeted dye and protein adsorption. *Journal of Applied Polymer Science,* 134(21), n/a-n/a.

Bugnicourt, L., & Ladavière, C. (2016). Interests of chitosan nanoparticles ionically cross-linked with tripolyphosphate for biomedical applications. *Progress in Polymer Science,* 60(Supplement C), 1-17.

Burkinshaw, S. M., & Salihu, G. (2018). The role of auxiliaries in the immersion dyeing of textile fibres: Part 10 the influence of inorganic electrolyte on the wash-off of reactive dyes. *Dyes and Pigments,* 149, 652-661.

Cao, C., Xiao, L., Chen, C., Shi, X., Cao, Q., & Gao, L. (2014). In situ preparation of magnetic Fe3O4/chitosan nanoparticles via a novel reduction–precipitation method and their application in adsorption of reactive azo dye. *Powder Technology,* 260, 90-97.

Chaudhari, A. U., Paul, D., Dhotre, D., & Kodam, K. M. (2017). Effective biotransformation and detoxification of anthraquinone dye reactive blue 4 by using aerobic bacterial granules. *Water Research,* 122, 603-613.

Cheung, W. H., Szeto, Y. S., & McKay, G. (2009). Enhancing the adsorption capacities of acid dyes by chitosan nano particles. *Bioresource Technology,* 100(3), 1143-1148.

Costa, E. M., Silva, S., Vicente, S., Neto, C., Castro, P. M., Veiga, M., . . . Pintado, M. M. (2017). Chitosan nanoparticles as alternative anti-staphylococci agents: Bactericidal, antibiofilm and antiadhesive effects. *Materials Science and Engineering: C,* 79, 221-226.

Galante, R., Rediguieri, C. F., Kikuchi, I. S., Vasquez, P. A. S., Colaço, R., Serro, A. P., & Pinto, T. J. A. (2016). About the Sterilization of Chitosan Hydrogel Nanoparticles. *PLoS ONE,* 11(12), e0168862.

Gan, Q., & Wang, T. (2007). Chitosan nanoparticle as protein delivery carrier—Systematic examination of fabrication conditions for efficient loading and release. *Colloids and Surfaces B: Biointerfaces,* 59(1), 24-34.

Georgiou, D., Melidis, P., Aivasidis, A., & Gimouhopoulos, K. (2002). Degradation of azo-reactive dyes by ultraviolet radiation in the presence of hydrogen peroxide. *Dyes and Pigments,* 52(2), 69-78.

Gullon, B., Montenegro, M. I., Ruiz-Matute, A. I., Cardelle-Cobas, A., Corzo, N., & Pintado, M. E. (2016). Synthesis, optimization and structural characterization of a chitosan-glucose derivative obtained by the Maillard reaction. *Carbohydr Polym,* 137, 382-389.

Haider, J., Majeed, H., Williams, P. A., Safdar, W., & Zhong, F. (2017). Formation of chitosan nanoparticles to encapsulate krill oil (Euphausia superba) for application as a dietary supplement. *Food Hydrocolloids,* 63, 27-34.

Hashad, R. A., Ishak, R. A. H., Fahmy, S., Mansour, S., & Geneidi, A. S. (2016). Chitosan-tripolyphosphate nanoparticles: Optimization of formulation parameters for improving process yield at a novel pH using artificial neural networks. *International Journal of Biological Macromolecules,* 86, 50-58.

Hebeish, A., Sharaf, S., & Farouk, A. (2013). Utilization of chitosan nanoparticles as a green finish in multifunctionalization of cotton textile. *International Journal of Biological Macromolecules,* 60(0), 10-17.

Hu, Z. G., Zhang, J., Chan, W. L., & Szeto, Y. S. (2006). The sorption of acid dye onto chitosan nanoparticles. *Polymer,* 47(16), 5838-5842.

ISO. (2009). Biological evaluation of medical devices *Tests for in vitro cytotoxicity* (Vol. ISO 10993-5:2009, p. 34). Geneva: International Organization for Standardization.

Jha, P., Jobby, R., & Desai, N. S. (2016). Remediation of textile azo dye acid red 114 by hairy roots of Ipomoea carnea Jacq. and assessment of degraded dye toxicity with human keratinocyte cell line. *Journal of Hazardous Materials,* 311, 158-167.

Joseph, J. J., Sangeetha, D., & Gomathi, T. (2016). Sunitinib loaded chitosan nanoparticles formulation and its evaluation. *International Journal of Biological Macromolecules,* 82, 952-958.

Khatri, A., Peerzada, M. H., Mohsin, M., & White, M. (2015). A review on developments in dyeing cotton fabrics with reactive dyes for reducing effluent pollution. *Journal of Cleaner Production,* 87, 50-57.

Kumar, A., Vimal, A., & Kumar, A. (2016). Why Chitosan? From properties to perspective of mucosal drug delivery. *International Journal of Biological Macromolecules,* 91, 615-622.

Kumar, S. P., Birundha, K., Kaveri, K., & Devi, K. T. R. (2015). Antioxidant studies of chitosan nanoparticles containing naringenin and their cytotoxicity effects in lung cancer cells. *International Journal of Biological Macromolecules,* 78, 87-95.

Loh, J. W., Schneider, J., Carter, M., Saunders, M., & Lim, L.-Y. (2010). Spinning Disc Processing Technology: Potential for Large-Scale Manufacture of Chitosan Nanoparticles. *Journal of Pharmaceutical Sciences,* 99(10), 4326-4336.

Lu, Y.-H., Chen, Y.-Y., Lin, H., Wang, C., & Yang, Z.-D. (2010). Preparation of chitosan nanoparticles and their application to Antheraea pernyi silk. *Journal of Applied Polymer Science,* 117(6), 3362-3369.

Luo, S., & Van Ooij, W. J. (2002). Surface modification of textile fibers for improvement of adhesion to polymeric matrices: a review. *Journal of Adhesion Science and Technology,* 16(13), 1715-1735.

Momenzadeh, H., Tehrani-Bagha, A. R., Khosravi, A., Gharanjig, K., & Holmberg, K. (2011). Reactive dye removal from wastewater using a chitosan nanodispersion. *Desalination,* 271(1), 225-230.

Nayak, M. C., Isloor, A. M., Moslehyani, A., Ismail, N., & Ismail, A. F. (2018). Fabrication of novel PPSU/ZSM-5 ultrafiltration hollow fiber membranes for separation of proteins and hazardous reactive dyes. *Journal of the Taiwan Institute of Chemical Engineers,* 82, 342-350.

Nogueira, D. R., Tavano, L., Mitjans, M., Pérez, L., Infante, M. R., & Vinardell, M. P. (2013). In vitro antitumor activity of methotrexate via pH-sensitive chitosan nanoparticles. *Biomaterials,* 34(11), 2758-2772.

Ramesh Kumar, A., & Teli, M. D. (2007). Electrokinetic studies of modified cellulosic fibres. *Colloids and Surfaces A: Physicochemical and Engineering Aspects,* 301(1), 462-468.

Robinson, T., McMullan, G., Marchant, R., & Nigam, P. (2001). Remediation of dyes in textile effluent: a critical review on current treatment technologies with a proposed alternative. *Bioresource Technology,* 77(3), 247-255.

Shahid ul, I., Shahid, M., & Mohammad, F. (2013). Green Chemistry Approaches to Develop Antimicrobial Textiles Based on Sustainable Biopolymers—A Review. *Industrial & Engineering Chemistry Research,* 52(15), 5245-5260.

Shahidi, S., Wiener, J., & Ghoranneviss, M. (2013). *Surface Modification Methods for Improving the Dyeability of Textile Fabrics*. In M. Gunay (Ed.), *Eco-Friendly Textile Dyeing and Finishing* (pp. 33-52): InTech

Shajahan, A., Shankar, S., Sathiyaseelan, A., Narayan, K. S., Narayanan, V., Kaviyarasan, V., & Ignacimuthu, S. (2017). Comparative studies of chitosan and its nanoparticles for the adsorption efficiency of various dyes. *International Journal of Biological Macromolecules,* 104, 1449-1458.

Smith, B. (2005). *Wastes from Textile Processing*. In *Plastics and the Environment* (pp. 243-309): John Wiley & Sons, Inc.

Tavaria, F. K., Soares, J. C., Reis, I. L., Paulo, M. H., Malcata, F. X., & Pintado, M. E. (2012). Chitosan: antimicrobial action upon staphylococci after impregnation onto cotton fabric. *J Appl Microbiol,* 112(5), 1034-1041.

Tissera, N. D., Wijesena, R. N., & de Silva, K. M. N. (2016). Ultrasound energy to accelerate dye uptake and dye–fiber interaction of reactive dye on knitted cotton fabric at low temperatures. *Ultrasonics Sonochemistry,* 29, 270-278.

Tsuboy, M. S., Angeli, J. P. F., Mantovani, M. S., Knasmüller, S., Umbuzeiro, G. A., & Ribeiro, L. R. (2007). Genotoxic, mutagenic and cytotoxic effects of the commercial dye CI Disperse Blue 291 in the human hepatic cell line HepG2. *Toxicology in Vitro,* 21(8), 1650-1655.

Wang, J. J., Zeng, Z. W., Xiao, R. Z., Xie, T., Zhou, G. L., Zhan, X. R., & Wang, S. L. (2011). Recent advances of chitosan nanoparticles as drug carriers. *Int J Nanomedicine,* 6, 765-774.

Wasim, M., Sagar, S., Sabir, A., Shafiq, M., & Jamil, T. (2017). Decoration of open pore network in Polyvinylidene fluoride/MWCNTs with chitosan for the removal of reactive orange 16 dye. *Carbohydrate Polymers,* 174, 474-483.

Wu, Y., Yang, W., Wang, C., Hu, J., & Fu, S. (2005). Chitosan nanoparticles as a novel delivery system for ammonium glycyrrhizinate. *International Journal of Pharmaceutics,* 295(1), 235-245.

Yang, H.-C., Wang, W.-H., Huang, K.-S., & Hon, M.-H. (2010). Preparation and application of nanochitosan to finishing treatment with anti-microbial and anti-shrinking properties. *Carbohydrate Polymers,* 79(1), 176-179.

Zhou, L., Jin, J., Liu, Z., Liang, X., & Shang, C. (2011). Adsorption of acid dyes from aqueous solutions by the ethylenediamine-modified magnetic chitosan nanoparticles. *Journal of Hazardous Materials,* 185(2), 1045-1052.